

Suspended Columns for Seismic Isolation in Structures (SCSI): Experimental and numerical studies

Ali Beirami Shahabi^{a1}, Gholamreza Zamani Ahari^{*1} and Majid Barghian^{b2}

¹Department of Civil Engineering, Faculty of Engineering, Urmia University, Urmia, Iran

²Faculty of Civil Engineering, University of Tabriz, Tabriz, Iran

(Received March 25, 2020, Revised May 20, 2020, Accepted June, 10, 2020)

Abstract. In this paper, a modified and improved seismic isolation system called suspension columns for seismic isolation was investigated. An experimental study of the proposed isolation method, together with theoretical and numerical analyses, has thoroughly been conducted. In the proposed method, during the construction of the foundation, some cavities are created at the position of the columns inside the foundation and the columns are placed inside the cavities and hanged from the foundation by flexible cables rather being directly connected to the foundation. Since the columns are suspended and due to the gap between the columns and walls of the cavities, the structure is able to move freely to each side thus, the transmitted seismic actions are reduced. The main parameter of this isolation technique is the length of the suspension cable. As the cable length is changed, the natural frequency of the structure is also changed, thus, the desired frequency can be achieved by means of an appropriate cable length. As the experimental phase of the study, a steel frame structure with two floors was constructed and subjected to the acceleration of three earthquakes using a shaking table with different hanging cable lengths. The structural responses were recorded in terms of acceleration and relative displacement. The experimental results were compared to the theoretical and numerical ones, obtained from the MATLAB programming and the finite element software ABAQUS, showing a suitable agreement between them. The results confirm the effectiveness of the proposed isolation method in reducing the seismic effects on the structure.

Keywords: seismic isolation; base isolation; suspended columns; passive control; cable hanger; shaking table test

1. Introduction

Nowadays, seismic isolation is one of the most common methods for seismic control of structures. In this method, the natural period of the structure is altered and transferred from the high-risk region to the low-risk one; therefore, the seismic response of the structure is reduced. To increase the structure period, various methods have been proposed. The idea of a soft first story is one of the proposed approaches to raise the natural period of the structure. Although some buildings were constructed by this idea at a time, the poor performance of this technique in the occurred earthquakes caused the construction of this type of structure to be ceased (Chopra *et al.* 1973). One of the other simplest and first isolation methods is the sliding technique wherein the structure foundation is mounted on a low-friction layer, which has been studied by several researchers, including Lu and Yang (1997). Nanda *et al.* (2012) performed a study on a sliding isolation system with natural stone as sliding support. They employed four different types of natural stone

including green marble as sliding interfaces. The experimental result showed that the coefficient of friction values of these interfaces lies in 0.05 to 0.15, which is appropriate for seismic protection so that it causes accelerations reduction up to 50%. Mokha *et al.* (1990) carried out a study on the sliding support manufactured using Teflon and proved the effectiveness of its application for seismic control of the structure. Further study on the Teflon support resulted in the innovation of the resilient sliding support by Mostaghel and Khodaverdian (1987). In this method, multiple Teflon layers are laid on each other and create a seismic isolation device. The aforementioned research methods were all on the flat sliding surface. One of the disadvantages of flat sliding support is the lack of capability of structure to restore to the initial position after earthquakes. Therefore, they embedded a rubber core inside the plates to supply the restoring force that enhanced the isolator performance. Uncertainty about the predicted performance and changes in the friction coefficient over time are among the drawbacks of the mentioned methods. Supplementary studies on the sliding isolation and the necessity of providing both reliable restoring force and energy dissipation at the same time led to the innovation of concave sliding isolators, so-called pendulum isolator, by Zayas *et al.* (1990). Furthermore, to enhance the performance, Fenz *et al.* (2006, 2008a, 2008c) converted this system to the double-pendulum and triple-pendulum by applying some changes to the system. Pranesh and Sinha (2000, 2002) introduced the variable-frequency isolator by

*Corresponding author, Assistant Professor

E-mail: g.zamani@urmia.ac.ir

^aPh. D. Student

E-mail: a.bayrami@urmia.ac.ir

^bAssociate Professor

E-mail: barghian@tabrizu.ac.ir

changing the curvature of the sliding surface. Xiong *et al.* (2017, 2018) made another innovation in this system by changing the sliding surface from the curved to the sloped version.

Among the other isolation methods, there are rolling-based techniques in which the rod or ball is placed beneath the structure to create the seismic isolation. Lin *et al.* (1995) suggested using circular rolling rods and Jangid (1998), Jangid and Londhe (1998) and Rawat *et al.* (2018) provided the restoring capability for the isolation system by changing the circular rod to an elliptical one. Ou *et al.* (2010) and Chen and Wang (2016) investigated the application of orthogonal rods to provide double-sided isolation on a sloped surface. Barghian and Shahabi (2007) introduced mushroom-shaped support beneath the structure. Ismail *et al.* (2009, 2012, 2016) suggested applying the roll-in-cage isolator.

Among other most-applied methods of seismic isolation are elastic layers-based approaches, where in the steel and rubber layers are laid on each other by some specific operations and produce the isolation block. This block offers high vertical stiffness and low lateral stiffness. To supply sufficient damping ratio in this type of isolator, Robinson and Tucker (1977) and Robinson (1982) put a lead core inside the isolator block. Many studies have been conducted so far on the seismic behavior of this type of isolator (Warn *et al.* 2007, Yamamoto *et al.* 2009, Kikuchi *et al.* 2010, Kumar *et al.* 2014 and Han and Warn 2014). Nowadays, this method is one of the most common seismic isolation approaches and further studies are being performed to introduce a more precise model to predict the seismic behavior of the isolation system. In addition to the conventional methods, some researchers have proposed some other innovative techniques. Karayel *et al.* (2017) proposed the ground-floor spring-equipped columns. Hosseini and Farsangi (2012) proposed the telescopic columns. Nakamura *et al.* (2011) presented the core-suspended structure whereby a concrete core is constructed in the middle of structure above which the main structure is suspended so that the structure vibrates freely to the sides once subjected to an earthquake.

All of the innovative seismic isolation methods have advantages and drawbacks and, therefore; further studies are needed to resolve the disadvantages of the current methods and to propose new methods in this scope.

Another method of seismic isolation is suspension-based methods. Some researchers have already worked on different types of suspension-based isolation systems which have been studied theoretically, experimentally, and some were implemented in practice. One has been applied to a 3-story building in Ashkhabad, Turkmenistan in 1959, (Eisenberg, 1992). In some of the proposed methods, rods from inside a larger circular column on the ground floor hang the building columns. The related document has been mentioned in Russian technical literature, (Eisenberg, 1983) and patented in Japan and Mexico. Also, Newmark and Rosenblueth (1971) have discussed this topic theoretically. Some doctoral dissertations studied this subject such as in Romania, which included shaking table tests (Al, E.A., 1992). In the proposed system, V shape members are

attached to columns while inverse V shape members are attached to the foundation. These members are hung from each other by suspension cable and create the isolation system. The disadvantage of this method is that an additional floor in the structure must be created for the isolation purpose, which leads to significant costs. Another model of this system was tested on a shaking table at the University of Illinois by Professor Foutch (1993). In this system, short hollow supports are installed on the foundation at the position of each column, and tensile cables hang inside the supports. As a series of experiments, a test specimen with a scale of one-eighth of the real structure was constructed and examined under the earthquake excitations. In the conducted tests, hanging cables with lengths of 8 and 26 inches were used. There are limitations to the study. In this system, it is possible to get a higher natural period by increasing the length of the cable but by doing that, the space occupied by the device on the ground floor increases, and the useful area of the floor will be limited. To solve the problem of space occupation and to achieve higher suspension length, a modified system is proposed by the authors. This isolation system called suspended columns for seismic isolation in structures (SCSI). In this method, useful space on the ground floor is increased and a larger natural period can be achieved. In the current study, taking into account the similarity laws, the suspension cable length up to 2 meters was tested which leads to the natural period up to 2.8 seconds which is far enough from the earthquake resonance zone. Moreover, various effective parameters in this isolation system including damping ratio and suspension cable length have been investigated and the study results have been obtained theoretically, experimentally, and numerically and compared with each other. In this way, the test scope of this study is larger than the previous studies, and the experiment can be performed more realistically.

The study of the SCSI isolation system was conducted in two phases. As the first phase, a preliminary simplified theoretical model along with the characteristic features of the system was introduced and discussed (Shahabi *et al.* 2019). As the second phase (present study), a laboratory prototype building made of a two-floor steel frame was constructed and the seismic performance of the isolation system was experimentally evaluated using shaking table tests.

2. Introduction of the suspended columns for seismic isolation in structures (SCSI)

In the proposed system, the building columns on the ground floor are connected to the foundation by suspension cables rather being directly connected to the foundation. During construction of the foundation, cavities - like elevator pits - are created in the location of columns inside the foundation and steel supports are installed at the upper part of the cavities. The suspension cables are hanged from these supports into the cavities and the columns are put into the cavities to the depth equal to the length of the cable. Steel plates with dimensions larger than the column are

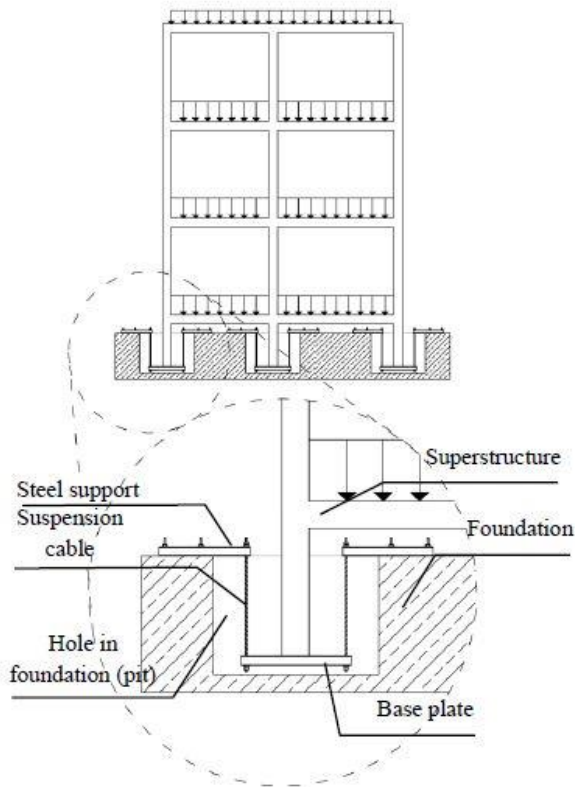


Fig. 1 The schematic view and detail of the suspended columns isolation system

installed at the end of each column and these plates are connected to the steel support at top of the cavities by suspension cables. Due to the flexibility of suspension cables and the gap between columns and cavities, the columns can easily move to the sides during an earthquake so that the seismic isolation is achieved. The schematic of the proposed method is shown in Fig. 1.

3. Experimental study

To validate the results of the theoretical study, a specimen of the isolated structure was constructed and the behavior of the proposed isolation system was experimentally evaluated using a shaking table test. The constructed prototype structure is made of steel frame with two floors, one for base covering and second for the roof of the structure. The dimensional similitude relations were applied for building this prototype. The details of the conducted experiments are described below.

3.1 Specifications of the specimen and test setup

3.1.1 Similitude law between model and prototype

The prototype was made of a $\frac{1}{2}$ scale relative to the real structure model. This structure was manufactured using a rectangular-box steel profile and included three main parts, namely foundation, structure, and damper. Appropriate dimensional similarity laws were considered in the

Table 1 Similitude law between model and prototype

| Physical parameters | Symbol | Similitude relations | Scale factor |
|---------------------|------------|----------------------|--------------|
| Length | L | λ^{-1} | 1/2 |
| Young's module | E | 1 | 1 |
| Density | ρ | 1 | 1 |
| Mass | M | λ^{-3} | 1/8 |
| Time | T | λ^{-1} | 1/2 |
| Acceleration | A | λ | 2 |
| Damping ratio | ξ | 1 | 1 |
| Damping | c | λ^{-2} | 1/4 |
| Frequency | ω_n | λ | 2 |
| Cable length | r | λ^{-2} | 1/4 |

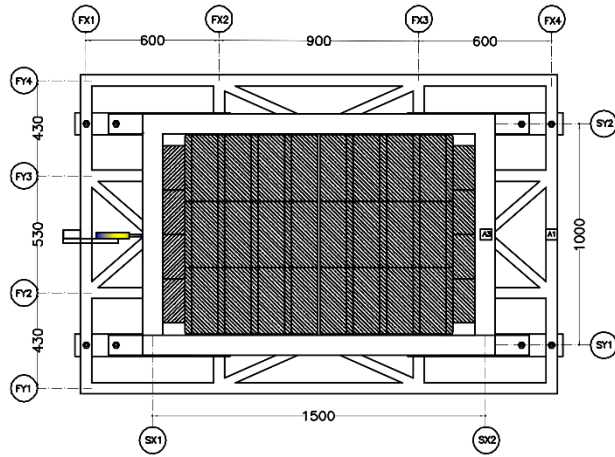
construction of laboratory sample components. Due to the dynamical nature of this experiment, the relevant rules were used. In Table 1 the similitude laws used in construction and testing are listed. These laws were employed in numerous similar shaking table tests such as Karayel *et al.* (2017).

3.1.2 Foundation

Instead of concrete foundation, to lighten the weight of the foundation and possibility of vibration on the shaking table, the foundation was made from the steel box profile with 5×5 cm dimensions and thickness of 2 mm. In the construction of the foundation, vertical components were employed in the corners of cavities with horizontal components being installed above and beneath them to provide the necessary integrity as well as the appropriate support to hang the suspension cables. Diagonal components were installed as braces in different directions to provide the horizontal and vertical rigidity so that the foundation could be assumed as a concrete foundation from the rigidity standpoint. Before construction, the rigidity and strength of the foundation were evaluated using SAP2000 software. Fig. 2 illustrates an image of the constructed prototype structure and foundation along with the schematic view, dimensions. As can be seen from the figure, the main structure is connected to the foundation using suspension cables made of steel wire rope.

3.1.3 Structure

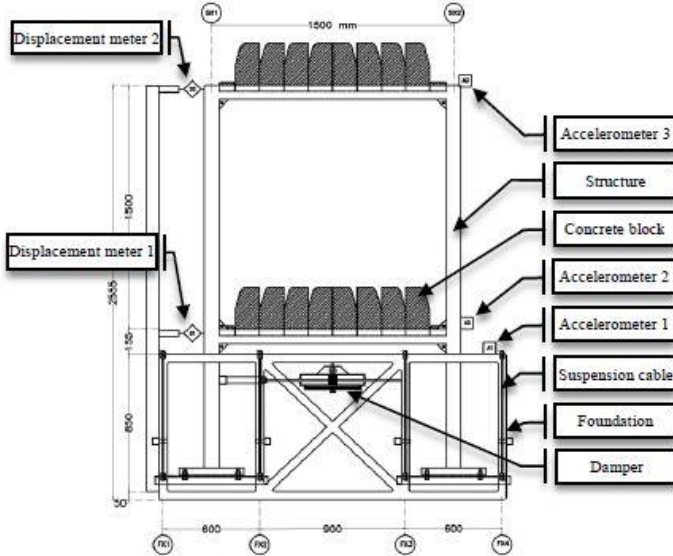
The members of the main structure were made of a square-box steel profile with 9×9 cm dimensions and 2 mm of thickness. This structure included two bottom and top floor, which has 120 cm length, 100 cm width, and 150 height plus 90 cm of column height inside the foundation. The floor of each story was fabricated from a 2 mm steel flat plate along with support beams on the beneath, made of steel tube 4×4 cm in dimensions, and 2 mm in thickness for flexural reinforcement. As can be observed from Fig. 2, to connect the structure to the foundation, a steel channel profile of grade 10 with a length of 60 cm was horizontally installed beneath each column. Two suspension cables with a diameter of 6 mm and length of 65 cm for each column - i.e. eight suspension cables for the entire structure - hanged the structure from the top of the foundation. To change the height of suspension cables, sliding support was installed



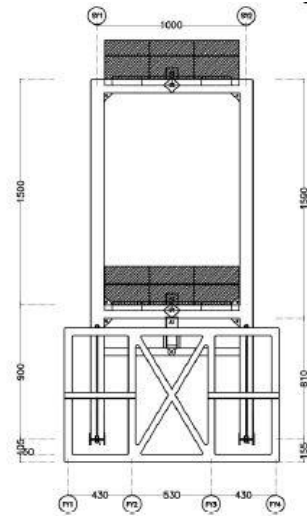
(a) plan view of the structure



(b) photo of the test steel frame on shaking table



(c) front view of the structure



(d) side view of the structure

Fig. 2 Photo and schematic view of the shaking table test setup (dimensions in mm)

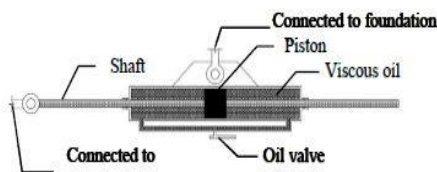
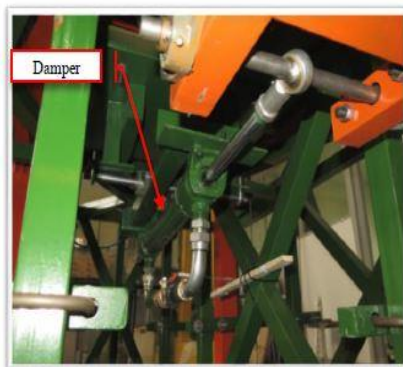


Fig. 3 The schematic view and a picture of the viscous damper used for the test

for each cable that slides over the cable to adjust the free vibrating length and to allow performing tests at different suspension lengths. Also, to investigate the effect of the earthquake on the non-isolated structure, the fixed-base structure was subjected to the earthquake accelerations wherein the structure base was directly connected to the foundation via the removal of the suspension cable and welding the structure to the foundation. The fabricated structure was a moment frame and the weight of the structural elements was 240 Kgf. To acquire extra load, concrete blocks were used. The weight of the concrete blocks was 720 Kgf in each story, the total weight of the structure was 1680 Kgf, and the foundation weight was 240 Kgf. Also, to protect the integrity of the specimen during shaking, the concrete blocks were fastened to each other and were connected to each floor by appropriate fasteners.

3.1.4 Damper

Proper damping is required to control and limit the displacement in the isolation systems. Therefore, a suitable

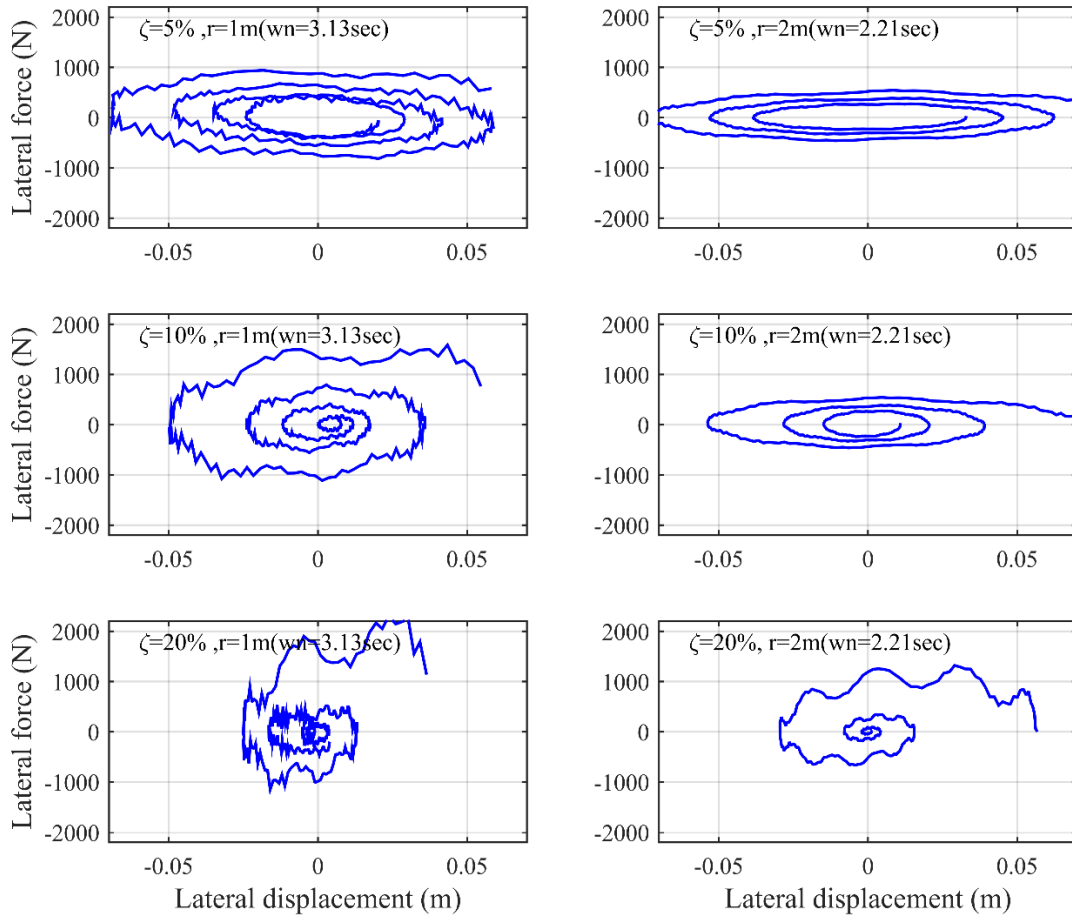


Fig. 4 Force-displacement diagram of the damper for 1, 2, 5 and 10 percent of damping ratio

damper was designed and fabricated for this system. The schematic view and a picture of the fabricated damper are shown in Fig. 3. By a forced vibration test applied to the constructed model and evaluating the time- amplitude graph, the inherent damping ratio of the system was estimated to be about 1%. Therefore, the use of external damper is necessary to provide enough damping. In the experiment, a viscous damper was used which was able to provide 3 to 100 percent damping ratios for the test model. To better understand the behavior of this system under different damping ratios, the force-displacement graphs for damping ratios of 1, 2, 5, and 10 percent were drawn in Fig. 4. Since the installed damper is a viscous type, the amount of damping produced depends on the loading velocity. It is well known that in earthquakes, the loading velocity is a random parameter. Therefore, initial displacement has been used to determine the energy absorption mechanism. The length of the hanging cable was 1 meter and the total mass of the structure was 1345.27 kg. In the evaluation, a relative displacement of 10 cm has been applied between the structure and the foundation and the force-displacement diagram has been drawn for various amounts of damping ratio.

As can be seen from Fig. 3, this damper is comprised of an oil cylinder, a piston, a shaft, and a valve. It works by moving hydraulic oil through a control valve based on

viscous damping wherein the hydraulic oil passes through the orifice to supply required damping. The orifice includes an adjustable valve to provide any desired damping ratio. The damper was connected to the foundation on the one side and to the structure on the other side. The damper dissipates energy by the relative motion of the structure to the foundation. When the valve is opened, the oil easily passes through it and produces small damping and when more damping is required, the valve is closed and larger damping is created in the system. It is worth noting that the investigation into the fabricated damper revealed that a portion of the achieved damping was frictional due to the presence of packing to avoid oil leakage. However, the contribution of this frictional damping is not noticeable compared to the viscous damping and can be neglected. Since the damper was equipped with a valve, it was possible to reach different values of damping ratios ranging from 3 to even 100 %. The damping ratios of 5, 10, and 20% were considered to perform tests.

3.1.5 Shaking table and data recording system

The shaking table available in the lab has dimensions of 2×3 m and weight-bearing capacity of 6 tons and is capable of supply the maximum acceleration, displacement, and frequency of $1g$, ± 10 cm, and 50Hz , respectively. This table provides a one-dimensional motion. The constructed structure was braced against the lateral motion

Table 2 Selected earthquake records for the shaking table test

| Record | M_s | d (km) | PGA (cm/s^2) | PGV (cm/s) | PGD (cm) |
|---|-------|-------------|----------------------------|--------------------------|-------------|
| El Centro 1940 | 6.95 | 6.1 | 312.7 | 36.1 | 21.3 |
| Peknold, N-S Kobe, Japan, 1995,Kak, 90 | 6.9 | 22.5 | 317.8 | 26.8 | 8.8 |
| Tabas, Iran, 1978,Tab, L | 7.35 | 1.79 | 837.8 | 98.8 | 37.5 |

During the test, one accelerometer was installed on the shaking table, one on the foundation, and two on each story of the structure in the middle of the cross beam of the story. To install displacement meters, since the relative displacement of the foundation and the structure was concerned, a vertical component made of steel rectangular box profile of 8×4 cm dimensions was mounted on the foundation vertically and the displacement sensors were installed to this component in the middle-level of each story. Since the displacement meters were connected to the foundation on the one side and to the structure on the other side, the relative displacement was measured during the vibration in each story. The comparison of the recorded acceleration on the shaking table and the foundation offered an acceptable agreement, implying the rigidity of the foundation. In Fig. 5, images of the accelerometer sensor and displacement meter used for data recording and their position are shown.

3.2 Specifications of earthquake records

To investigate the structural behavior under earthquake, the record of three earthquakes were used. The characteristics of these earthquakes are listed in Table 2.

4. Numerical study

ABAQUS finite element software was utilized for numerical modeling of the isolated structure. The beam element of B31 selected for modeling the structure members. The structural mass was divided into eight-part and placed in nodes. The axial dashpot element was assigned for the damper model. Also, the linear axial connector element was utilized for the suspension cable model.

5. Results and discussion

The isolated structure was subjected to the accelerations of three earthquakes and the results were recorded as the acceleration and relative displacement time-history responses of the isolated system. In the conducted experiments, the structure response was examined with two main variables, namely the length of the suspension cable and the damping ratio of the system. As the theoretical study, the structure was modeled as a mass-spring-damper system and the structural response was evaluated for different cable lengths at the damping ratios of 5, 10, 20 %, and the results were obtained as the response spectrum of pseudo-acceleration and relative displacement of the structure. In addition to the theoretical study, the numerical study was also conducted wherein the structure with real geometry and material specifications was analyzed in the same condition of the tests. The obtained results were plotted as the time- history of acceleration and relative displacement for each story with the cable lengths of 80, 100, 150, and 200 cm and at the damping ratios of 5, 10, and 20%. It should be noted that considering the laws of

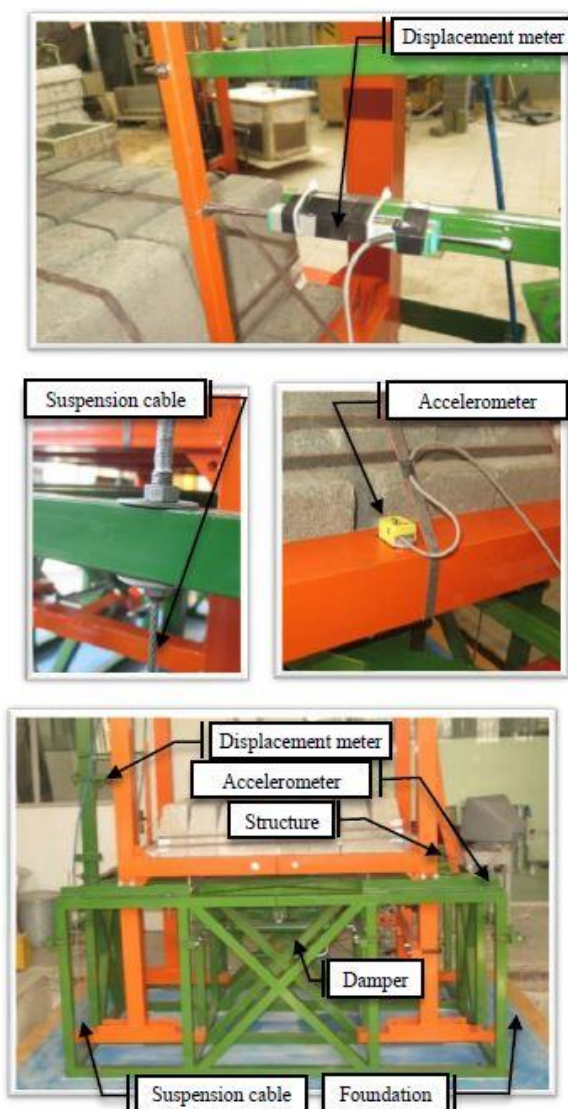
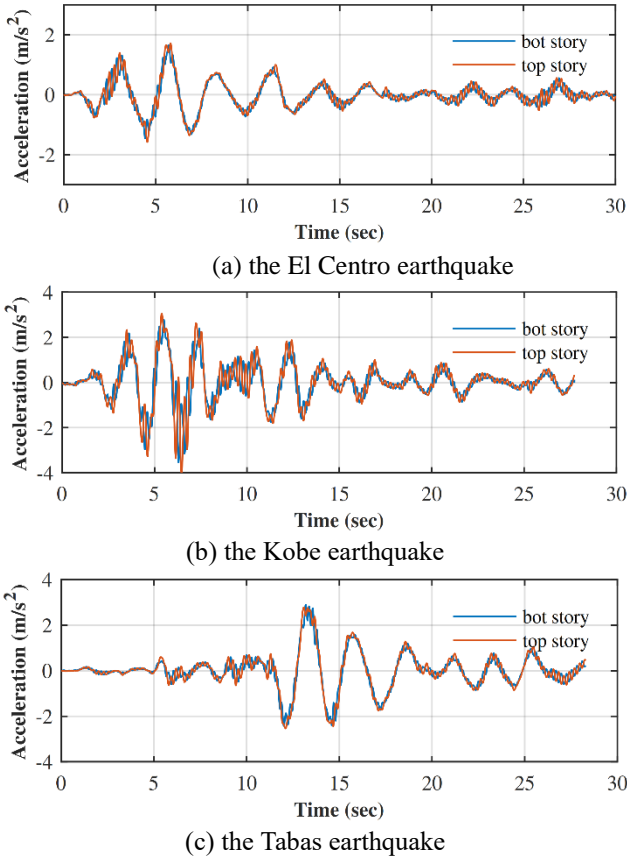


Fig. 5 Details of shaking table test setup

by four rollers to move merely across the shaking table moving direction. To perform this test, four accelerometer sensors and two displacement meters were employed. In Fig. 2, the square shapes stand for the accelerometer sensors and the diamond shape stands for displacement meters.



similitude, the one-fourth of the cable length values were used in the tests. The results of the experiments showed that after the earthquake excitation, no relative displacement was observed in the system and the structure returned to its original position. In this way, one of the major problems in the current seismic isolation methods will be solved. The obtained results are explained in some parts as follows. Lack of permanent displacement in the system indicates that the performance of the pendant cable is elastic and the damping caused by the structure and damper is quite viscous. In some isolation systems, yielding or frictional dampers may be used. Given the nature of these dampers, some permanent displacement may occur in this system after an earthquake; in this case, the damper must be replaced or restored after the earthquake. The construction and testing of the specimen of the proposed isolation system showed that the implementation of the system is practical and the construction process does not require high technology and this isolation system can be created at a reasonable cost. The simplicity of the proposed system raises the reliability of its proper function in earthquakes and minimizes the need for its service maintenance over time. One of the most commonly encountered problems with other common isolation systems is the loss of performance of isolators over time. The simplicity of the mechanism of the proposed system increases the reliability of its long-term proper performance.

The results of the conducted experiments are categorized into several sections, which are described as follows.

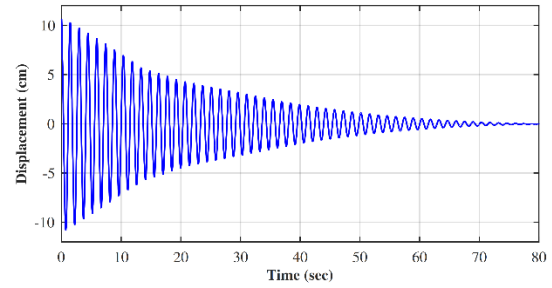


Fig. 7 Free vibration displacement response time-history of the test specimen without external damper

5.1 Comparison of the experimental accelerations recorded at the two levels of the structure floors

As it was already stated, to obtain the equation of motion, the lateral stiffness of the isolation system was assumed negligible in comparison with the lateral stiffness of the structural frame. Also, the structure frame was assumed rigid so the entire system was modeled as the concentrated mass-spring and damper. To control the validity of this assumption, one can compare the differences between the accelerations recorded at the two levels of the structure floors. Fig. 6 shows the recorded acceleration at the two-floor levels for the cable length of 150 cm and a damping ratio of 10% for the El Centro, Kobe, and Tabas earthquakes. As shown in the figure, the recorded accelerations are almost identical in the two upper and lower floors. This indicates that these two points moved together which approved the suitable precision of the rigidity assumed in the theoretical solution of the problem.

5.2 Measurement of the inherent damping ratio of the structure

To determine the inherent damping ratio of the system, the external damper was removed from the test structure and the inherent damping ratio was obtained of about 1.0%. This value was obtained experimentally by the free vibration and descending trend of vibration amplitude using the formulation associated with the damping ratio Fig. 7 demonstrates the time-history of the free vibration of the structure without the external damper using the initial displacement of 11 cm and the suspension cable length of 50 cm. This cable length causes the natural frequency of the structure to be 1.42 seconds. As can be observed from Fig. 7, the system without the external damper offers a low value of damping ratio so that the vibration is dissipated and decayed after a noticeably long time. Furthermore, the decreasing trend of the vibration amplitude shown in the figure is approximately exponential indicating that the damper exhibits an almost viscous behavior.

5.3 Experimental and numerical acceleration and displacement responses of the structure

Table 3 shows the maximum displacement and acceleration values generated in the structure for the three

Table 3 Comparison of the maximum displacement and acceleration values for three earthquakes, obtained by shaking table test and FEM analysis

| Record | Cable length ,cm | Damping ratio,% | Max disp., cm | | Difference % | Max Acc., m/s ² | | Difference % |
|-----------|------------------|-----------------|---------------|------|--------------|----------------------------|------|--------------|
| | | | Shake table | FEM | | Shake table | FEM | |
| El centro | 80 | 5 | 15.6 | 12.6 | 19% | 1.93 | 1.5 | 22% |
| | 100 | 5 | 16.1 | 14.4 | 11% | 1.92 | 1.46 | 24% |
| | 150 | 5 | 27.6 | 26.8 | 3% | 2.02 | 1.76 | 13% |
| | 200 | 5 | 26 | 28.4 | 9% | 1.35 | 1.42 | 5% |
| | 150 | 10 | 22.1 | 21.5 | 3% | 1.72 | 1.49 | 13% |
| | 150 | 20 | 15.2 | 15 | 1% | 1.62 | 1.16 | 28% |
| Kobe | 80 | 5 | 22.6 | 24.4 | 8% | 2.45 | 2.6 | 6% |
| | 100 | 5 | 20.5 | 21.4 | 4% | 2.12 | 2.16 | 2% |
| | 150 | 5 | 14.8 | 14.5 | 2% | 0.91 | 0.96 | 5% |
| | 200 | 5 | 12.5 | 12.4 | 1% | 0.69 | 0.62 | 10% |
| | 150 | 10 | 11.3 | 12.7 | 12% | 0.72 | 0.85 | 18% |
| | 150 | 20 | 10 | 10 | 0% | 0.7 | 0.71 | 1% |
| Tabas | 80 | 5 | 50.6 | 42.1 | 17% | 5.9 | 4.4 | 25% |
| | 100 | 5 | 59.4 | 51.7 | 13% | 5.29 | 4.55 | 14% |
| | 150 | 5 | 60.6 | 54 | 11% | 4.08 | 3.33 | 18% |
| | 200 | 5 | 64 | 68.5 | 7% | 3.33 | 3.2 | 4% |
| | 150 | 10 | 49.1 | 46.9 | 4% | 3.5 | 3 | 14% |
| | 150 | 20 | 19.1 | 46.9 | 146% | 3.38 | 2.95 | 13% |

earthquakes, and the results of the shaking table test and FEM software are compared. It should be noted that in the three aforementioned earthquakes, in damping ratio of 5% the cable lengths of 80, 100, 150, and 200 cm have been tested but due to laboratory limitations for 10% and 20% damping ratios, only cable length of 150 cm was tested and compared. Also, to show the time-history diagram of structural response, some examples of the acceleration and displacement time-history responses of the system obtained by the experimental and numerical methods for the El Centro, Kobe, and Tabas earthquakes are compared with each other in Fig. 8. As can be observed from Table 3 and Fig.8, the numerical results agree well with the experimental ones. From the acceleration time-history diagram, it is evident that small vibrations occurred in the general oscillation path of the structure is attributed to the free vibration of the structure itself. The vibration of the isolated structure can be considered as the vibration of a mass connected to two stiff and soft series of springs, the stiff spring represents the structure itself while the soft spring represents the suspension cable. After the vibration of the foundation, a combination of high-frequency (related to the structure itself) and the low-frequency (related to the suspension cable) vibrations occurred in the structure.

It is worth noting that in shaking table test results, a portion of the high frequencies was filtered employing MATLAB software to provide a smoother path in the diagrams

From acceleration and displacement time-history graphs, it can be seen that the maximum acceleration that occurred in the structure is decreased by increasing the suspension cable length. For instance, the maximum acceleration is 14 m/s^2 in the El Centro earthquake for the fixed-base case; while it decreases to 1.8 m/s^2 using the proposed isolation system for the cable length of 100 cm

and damping ratio of 5%. Furthermore, by increasing the cable length to 200 cm, the acceleration decreases to 1.3 m/s^2 , (Fig. 8). The variation trend of the maximum acceleration by increasing the suspension cable length was not uniform, i.e., the acceleration reduction was rapid by increasing the cable length up to 100 cm and after which this process gets slower. On the other hand, increasing the cable length, the relative displacement between the structure and foundation increases from zero in the fixed-base case to 13 cm and 29 cm at the cable lengths of 80 cm and 200 cm, respectively, (Fig. 8). However, this displacement occurs between the structure and foundation, and the structure drift (the main factor in the generation of stress in the structure components) is substantially negligible. To comply with the restrictions imposed by the building codes, the relative displacement must be limited to the permitted range.

5.4 Comparison of the maximum theoretical, numerical, and experimental response values of the structure

In the present study, the maximum values of displacement and acceleration responses of the structure were obtained through the theoretical, numerical, experimental (shaking table) studies, and comparison was made between them, and the results were listed in Table 4. In this table, the maximum values of the displacement and acceleration responses of a SDOF structure for the damping ratio of 5% at the cable lengths of 80, 100, 150, and 200 cm are presented. There is a good agreement between the results obtained from three studies but a difference of less than 10% can be observed between them. This difference can emerge from some sources. The existence of some constructional errors in prototype structure can affect the results of the experimental data. The combination of two

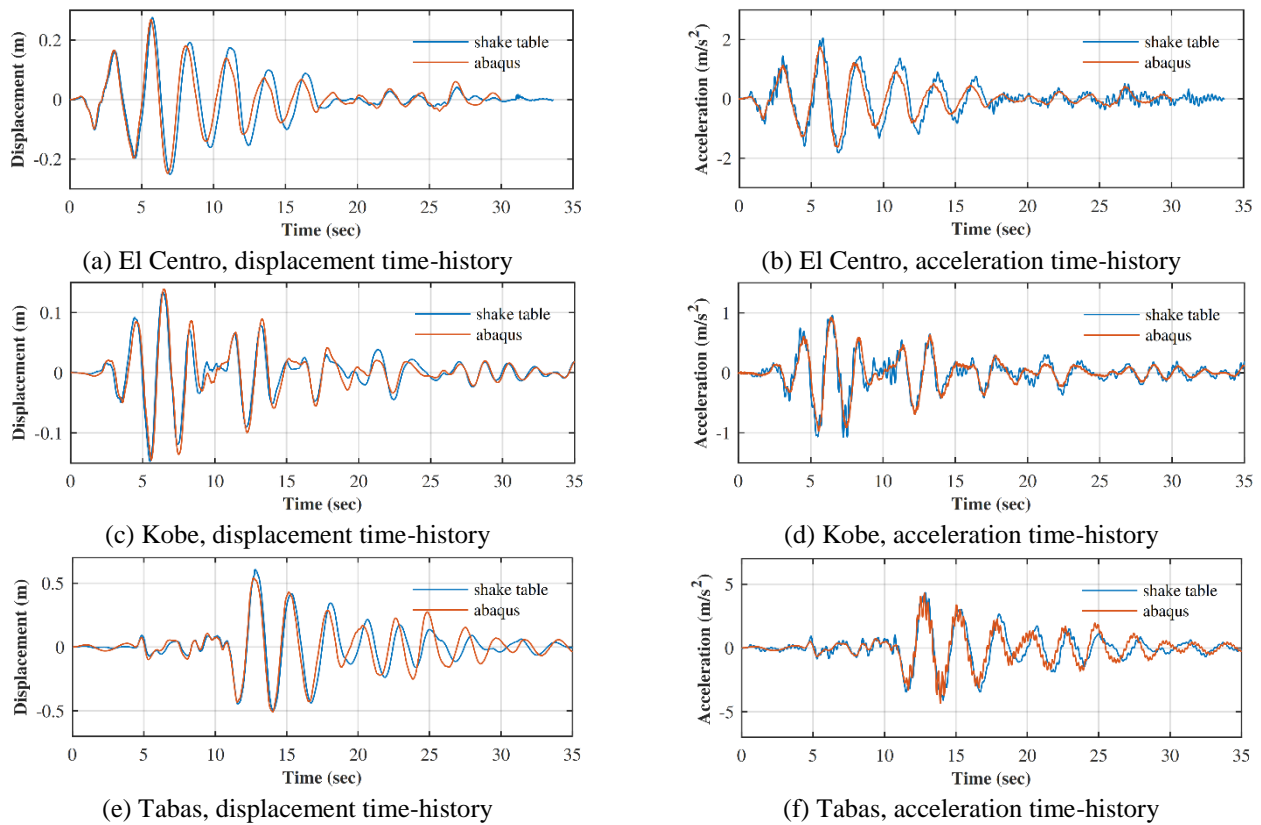


Fig. 8 Comparison of the acceleration and displacement time-history responses of shaking table test and finite element analysis result for the three earthquakes at cable lengths of 150 cm and damping ratio of 5%

Table 4 Comparison of the maximum of displacement and pseudo-acceleration of the isolated structure obtained by experimental, theoretical, and numerical methods, cable lengths of 80, 100, 150, and 200 cm and damping ratio of 5%

| Record | Source | Max displacement, cm | | | | Max Acceleration, m/s ² | | | |
|-----------|--------|----------------------|------|------|------|------------------------------------|------|------|------|
| | | r, cm | | | | r, cm | | | |
| | | 80 | 100 | 150 | 200 | 80 | 100 | 150 | 200 |
| El Centro | test | 15 | 16 | 27.5 | 24 | 1.9 | 1.9 | 2 | 1.3 |
| | FEM | 13 | 14.5 | 28 | 29 | 1.5 | 1.5 | 1.8 | 1.4 |
| | Matlab | 12 | 14 | 26 | 29 | 1.55 | 1.35 | 1.65 | 1.45 |
| Kobe | test | 23 | 23.4 | 14.7 | 12.5 | 2.7 | 2.1 | 1.1 | 0.73 |
| | FEM | 30 | 24.5 | 14.5 | 12.5 | 3 | 2.4 | 1 | 0.7 |
| | Matlab | 31 | 27 | 15 | 13 | 3.8 | 2.7 | 1 | 0.6 |
| Tabas | test | 51 | 60 | 60 | 62 | 6.4 | 6 | 4.3 | 3.1 |
| | FEM | 42 | 53 | 58 | 64 | 6 | 5.9 | 4.2 | 3.2 |
| | Matlab | 42 | 54 | 56 | 69 | 5.1 | 5.15 | 3.5 | 3.4 |

types of damping- viscous and Coulomb - in the structure, while there is only viscous damping incorporated in the numerical and theoretical modeling can be the other reason for these differences. Although the motion of the structure perpendicular to the earthquake acceleration direction was restrained by the rollers, the presence of some small movements perpendicular to the excitation direction and consequently the friction of these rollers can cause some error in the experimental results

Some simplifications made in the theoretical modeling compared to the numerical study such as the assumption of the rigid structure in the theoretical method can cause a slight difference between the results of two modeling methods.

Despite the existence of some small differences between the results of three studies, the overall comparison of the results reveals a suitable matching between them, implying the efficiency of the proposed isolation system in reducing the impact of earthquakes on the isolated structures from both experimental and analytical viewpoints.

5.5 Effect of damping on the seismic behavior of the system

To control the relative displacement, it is efficient to use an external damper. In the present study, a viscous damper was employed and the response of the structure was examined for the damping ratios of 5, 10, and 20% for

Table 5 Comparison of damping effect on the displacement and acceleration response of structure for 5, 10 and 20% damping ratio with a cable length of 150 cm for the shaking table test and FEM results

| Record | Damping ratio, % | Displacement | | | | Acceleration | | | |
|-----------|------------------|---------------|------|---|-----|----------------------------|------|---|-----|
| | | Max disp., cm | | Reduction compared to 5 % damping ratio | | Max Acc., m/s ² | | Reduction compared to 5 % damping ratio | |
| | | Test | FEM | Test | FEM | Test | FEM | Test | FEM |
| El Centro | 5 | 27.6 | 26.8 | - | - | 2.02 | 1.76 | - | - |
| | 10 | 22.1 | 21.5 | 20% | 20% | 1.72 | 1.49 | 15% | 15% |
| | 20 | 15.2 | 15 | 45% | 44% | 1.62 | 1.16 | 20% | 34% |
| Kobe | 5 | 14.8 | 14.5 | - | - | 0.91 | 0.96 | - | - |
| | 10 | 11.3 | 12.7 | 24% | 12% | 0.72 | 0.85 | 21% | 11% |
| | 20 | 10 | 10 | 32% | 31% | 0.7 | 0.71 | 23% | 26% |
| Tabas | 5 | 60.6 | 54 | - | - | 4.08 | 3.33 | - | - |
| | 10 | 49.1 | 46.9 | 19% | 13% | 3.5 | 3 | 14% | 10% |
| | 20 | 19.1 | 46.9 | 68% | 13% | 3.38 | 2.95 | 17% | 11% |

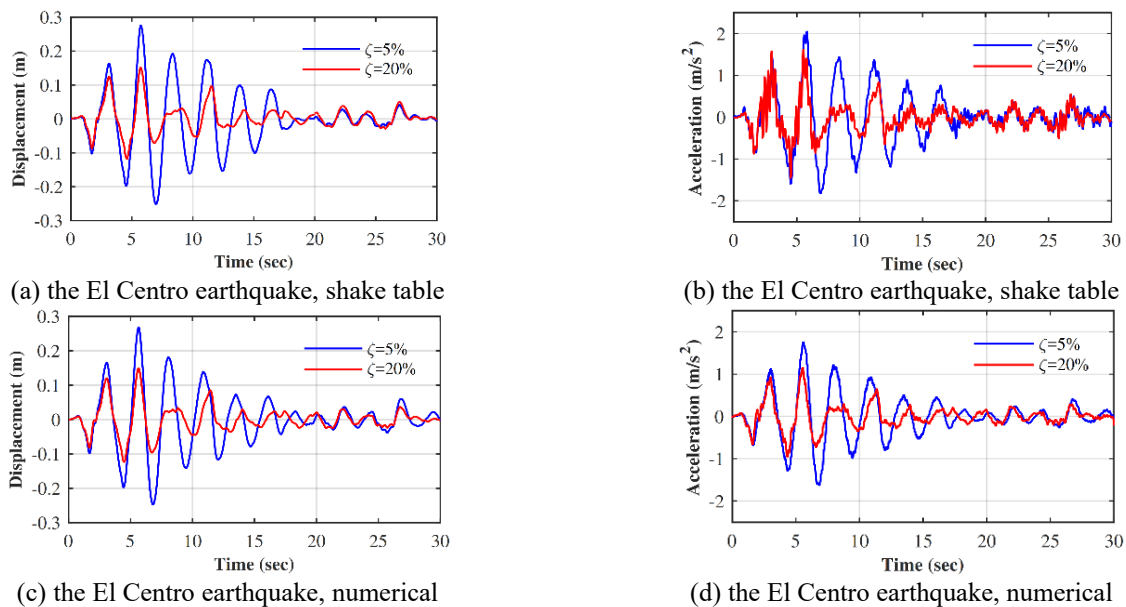


Fig. 9 Comparison of the displacement and acceleration time-history responses of structure using shake table test and finite element analysis, damping ratios of 5 and 20 %, and cable length of 150 cm

various suspension cable lengths. To evaluate the effect of damping ratio on the seismic behavior of the system, structure obtained by the experiment and numerical modeling were obtained and the maximum displacement and acceleration values of the structure under different earthquakes obtained from experiment and FEM analysis are compared in Table 5. Also, for a better explanation of the behavior of the structure, the acceleration and displacement time-history responses of the isolated structure, with damping ratios of 5 and 20 % and the cable length of 1.5 m for the El Centro earthquake were plotted in Fig. 9. As can be seen from the figure and Table 5, the growth of the damping ratio leads to a decrease in the acceleration and displacement of the isolated structure. Furthermore, the diagrams obtained from the experimental results agree well with the numerical results. The study on the damping at different cable lengths reveals that the effect of damping is more beneficial in shorter suspension cables lengths. In other words, the damping variations are more influential in high-frequency structures.

6. Conclusion

In the present study, the isolation system called suspended columns for seismic isolation (SCSI) was experimentally investigated. To evaluate the seismic performance of the isolation system, a steel moment frame structure with two floors was constructed by the scale factor of one-half of a real structure. Considering the capacity of the shaking table and the high weight of a concrete foundation, a steel foundation was built. To connect the main structure to the foundation and to create the isolation capability, suspension cables were utilized. The cables hung the structure like a pendulum into the holes inside the foundation. Due to the flexibility of the pendant cables, the relative movement of the foundation and the structure was provided. In order to conduct the tests with different cables lengths, movable supports were installed on the foundation. Since the application of an external damping system is beneficial to the proposed isolation method, an adjustable viscous damper was fabricated and mounted on the

structure to supply the required damping ratios. This damper was connected to the foundation on one side and to the structure on the other side and energy was dissipated during the relative movement of the structure and foundation. Three different earthquake records were used for shaking table tests. The acceleration and the relative displacement of the structure were recorded at different places in the structure. The experimental results were examined and compared with the theoretical results obtained from the MATLAB program and the numerical results of the ABAQUS finite element software. The comparison of the results showed that the results of the three studies are in good agreement and revealed that the application of the proposed isolation system is effective in the reduction of the seismic effects on the structure. The small differences between the results are justified by considering the simplifying assumptions and some minor errors in the construction of the specimen structure.

In the current study, two main variables affecting the performance of the system were examined. The suspension cable length and the damping ratio of the system. The seismic response of the structure was investigated at various cable lengths, with and without isolation system and with different damping ratios. Any change in the cable length led to a change in the natural frequency of the isolated structure so the more the cable length is, the longer the natural period of the structure will be. Moreover, it was observed that increasing the suspension cable length reduces the acceleration transmitted to the structure. It was also found out that increasing the cable length is effective up to some extent and after that; the increase in the cable length has less effect on reducing the acceleration transmitted to the structure.

It should be noted that increasing the suspension cable length, increases the relative displacement of the system as well. Therefore, an optimum length of the cable should be adopted to minimize the acceleration and relative displacement of the isolated structure and keep them at an acceptable level, simultaneously.

The study of the impact of damping on the performance of the system showed that damping is efficient in the reduction of the seismic response of the isolated structure, especially in shorter suspension cable lengths i.e. in structures with higher natural frequencies. Also, it was found out that increasing the damping ratio of the system reduces the acceleration and displacement all at once.

In summary, the following results can be stated for the current study:

- The results of the experimental, theoretical, and numerical studies proved the efficiency of the proposed isolation system in controlling the earthquake effects on the isolated structure.
- No residual relative displacement remains in the system. One of the main problems of the other seismic isolation methods is solved in this way.
- An optimum length of the suspension cable should be adopted to minimize the acceleration and relative displacement of the isolated structure.
- To eliminate the permanent displacement in the structure, a supplementary viscous damper should be

employed in the system. If a yielding damper is used, to remove the post-earthquake residual displacements, the damper should be restored or replaced.

- The application of an external damper to the system could significantly reduce the dynamic response of the structure, especially in shorter suspension cable lengths.
- The conducted experiments showed that the use of the system is feasible and can be practically applied for seismic isolation of buildings.

Simplicity, easy maintenance, and reliable performance of the system were approved through the experimental and analytical studies.

References

- Al, E.A.F.M.H. (1992), "Metode și procedee de izolare a fundațiilor la acțiuni dinamice", Ph.D. Dissertation, Tehnica Cluj-Napoca, Romania, (in Romanian).
- Barghian M. and Shahabi A.B. (2007), "A new approach to pendulum base isolation", *Struct. Control Hlth Monit.*, **14**, 177-85. <https://doi.org/10.1002/stc.115>.
- Chen, P.C. and Wang, S.J. (2016), "Improved control performance of sloped rolling-type isolation devices using embedded electromagnets", *Struct. Control Hlth. Monit.*, **24**(1), 1853. <https://doi.org/10.1002/stc.1853>.
- Chopra, A.K., Clough, D.P. and Clough, R.W. (1973), "Earthquake resistance of buildings with a 'soft' first storey", *Earthq. Eng. Struct. Dyn.*, **1**, 347-355. <https://doi.org/10.1002/eqe.4290010405>.
- Eisenberg, J.M., Melentyev, A.M., Smirnov, V.I. and Nemykin, A.N. (1992), "Applications of seismic isolation in the USSR". *In the Proc. 10th WCEE*, Madrid
- Eisenberg, J.M. (1983). Сейсмоизоляция и адаптивные системы сейсмозащиты. Изд-во "Наука". (in Russian).
- Fenz, D.M. and Constantinou, M.C. (2006), "Behaviour of the double concave Friction Pendulum bearing", *Earthq. Eng. Struct. Dyn.*, **35**, 1403-24. <https://doi.org/10.1002/eqe.589>.
- Fenz, D.M. and Constantinou, M.C. (2008a), "Modeling triple friction pendulum bearings for response-history analysis", *Earthq. Spectra*, **24**, 1011-1128. <https://doi.org/10.1193/1.2982531>.
- Fenz, D.M. and Constantinou, M.C. (2008b), "Spherical sliding isolation bearings with adaptive behavior: Theory." *Earthq. Eng. Struct. Dyn.*, **37**, 163-183. <https://doi.org/10.1002/eqe.750>.
- Foutch, D.A., Gambill, J.B. and Garza-Tamez, F. (1993). "Investigation of a seismic base isolation system based on pendular action", University of Illinois Engineering Experiment Station. College of Engineering. University of Illinois at Urbana-Champaign.
- Han, X. and Warn, G.P. (2014), "Mechanistic model for simulating critical behavior in elastomeric bearings", *J. Struct. Eng.* **141**(5), 40. [https://doi.org/10.1061/\(ASCE\)St.1943-541x.0001084](https://doi.org/10.1061/(ASCE)St.1943-541x.0001084).
- Hosseini, M. and Farsangi, E.N. (2012), "Telescopic columns as a new base isolation system for vibration control of high-rise buildings", *Earthq. Struct.*, **3**(6), 853-867. <https://doi.org/10.12989/eas.2012.3.6.853>.
- Ismail, M. (2016), "Novel hexapod-based unidirectional testing and FEM analysis of the RNC isolator", *Struct. Control Hlth. Monit.*, **23**, 894-922. <https://doi.org/10.1002/stc.1817>.
- Ismail, M., Rodellar, J. and Ikhoulane, F. (2009), "Performance of structure-equipment systems with a novel roll-n-cage isolation bearing", *Comput. Struct.*, **87**, 1631-1646. <https://doi.org/10.1016/j.compstruc.2009.09.006>.

- Ismail, M., Rodellar, J. and Ikhouane, F. (2012), "Seismic protection of low- to moderate-mass buildings using RNC isolator", *Struct. Control Health Monit.*, **19**, 22-42. <https://doi.org/10.1002/stc.421>.
- Jangid R.S. (2000), "Stochastic seismic response of structure isolated by rolling rods", *Eng. Struct.*, **22**, 937-946. [https://doi.org/10.1016/S0141-0296\(99\)00041-3](https://doi.org/10.1016/S0141-0296(99)00041-3).
- Jangid, R.S. and Londhe, Y.B. (1998), "Effectiveness of elliptical rolling rods for base isolation", *J. Struct. Eng. (ASCE)*, **124**, 469-472. [https://doi.org/10.1061/\(ASCE\)0733-9445\(1998\)124:4\(469\)](https://doi.org/10.1061/(ASCE)0733-9445(1998)124:4(469)).
- Karayel, V., Yuksel, E., Gokce, T. and Sahin, F. (2017), "Spring tube braces for seismic isolation of buildings", *Earthq. Eng. Eng. Vib.*, **16**, 219-31. <https://doi.org/10.1007/s11803-017-0378-9>.
- Kikuchi, M., Nakamura, T. and Aiken, I.D. (2010), "Three-dimensional analysis for square seismic isolation bearings under large shear deformations and high axial loads", *Earthq. Eng. Struct. Dyn.* **39**, 1513-1531. <https://doi.org/10.1002/eqe.1042>.
- Kumar, M., Whittaker, A.S. and Constantinou, M.C. (2014), "An advanced numerical model of elastomeric seismic isolation bearings", *Earthq. Eng., Struct., Dyn.*, **43**(13), 1955-1974. <https://doi.org/10.1002/eqe.2431>.
- Lin, T.W., Chern, C.C. and Hone, C.C. (1995), "Experimental study of base isolation by free rolling rods", *Earthq. Eng. Struct. Dyn.*, **24**, 1645-1650. <https://doi.org/10.1002/eqe.4290241207>.
- Lu, L. Y. and Yang, Y.B. (1997), "Dynamic response of equipment in structures with sliding support", *Earthq. Eng. Struct. Dyn.*, **26**(1), 61-76. [https://doi.org/10.1002/\(SICI\)1096-9845\(199701\)26:1](https://doi.org/10.1002/(SICI)1096-9845(199701)26:1).
- Mokha, A., Constantinou, M. and Reinhorn, A. (1990), "Teflon bearings in base isolation I: Testing", *J. Struct. Eng.*, **116**, 438-54. [https://doi.org/10.1061/\(ASCE\)0733-9445\(1990\)116:2\(438\)](https://doi.org/10.1061/(ASCE)0733-9445(1990)116:2(438)).
- Mostaghel N. and M. Khodaverdian (1987), "Dynamics of resilient-friction base isolator (R-FBI)", *Earthq. Eng. Struct. Dyn.*, **15**, 379-90. <https://doi.org/10.1002/eqe.4290150307>.
- Nakamura, Y., Saruta, M., Wada, A., Takeuchi, T., Hikone, S. and Takahashi, T. (2011), "Development of the core-suspended isolation system", *Earthq. Eng. Struct. Dyn.*, **40**, 429-447. <https://doi.org/10.1002/eqe.1036>.
- Nanda, R.P., Agarwal, P. and Shrikhande, M. (2012) "Suitable friction sliding materials for base isolation of masonry buildings", *Shock Vib.*, **19**, 1327-1339. <http://dx.doi.org/10.1155/2012/106436>.
- Newmark, N. (1971). "Rosenblueth, "Fundamentals of Earthquake Engineering", In: Prentice Hall, Eaglewood Cliffs, New Jersey.
- Ou, Y.C., Song, J. and Lee, G.C. (2010), "A parametric study of seismic behavior of roller seismic isolation bearings for highway bridges", *Earthq. Eng. Struct. Dyn.* **39**, 541-559. <https://doi.org/10.1002/eqe.958>.
- Pranesh M. and Ravi S. (2002), "Earthquake resistant design of structures using the variable frequency pendulum isolator", *J. Struct. Eng.*, **128**(7), 870-880. [https://doi.org/10.1061/\(ASCE\)0733-9445\(2002\)128:7\(870\)](https://doi.org/10.1061/(ASCE)0733-9445(2002)128:7(870)).
- Pranesh M. and Sinha R. (2000), "VFPI: An isolation device for aseismic design", *Earthq. Eng. Struct. Dyn.*, **29**(5), 603-627. [https://doi.org/10.1002/\(SICI\)1096-9845\(200005\)29:5](https://doi.org/10.1002/(SICI)1096-9845(200005)29:5).
- Rawat, A., Ummer, N. and Matsagar, V. (2018), "Performance of bi-directional elliptical rolling rods for base isolation of buildings under near-fault earthquakes", *Advan. Struct. Eng.*, **21**(5), 675-693. <https://doi.org/10.1177/1369433217726896>.
- Robinson, W.H. (1982), "Lead-rubber hysteretic bearings suitable for protecting structures during earthquakes", *Earthq. Eng. Struct. Dyn.* **10**, 593-604. <https://doi.org/10.1002/eqe.4290100408>.
- Robinson, W.H. and Tucker, A.G. (1977), "A lead-rubber shear damper", *Bull. N. Z. Natl. Soc. Earthq. Eng.* **3**, 93-101.
- Shahabi, A.B., Ahari, G.Z. and Barghian, M. (2019), "Suspended columns for seismic isolation in structures (SCSI): A preliminary analytical study", *Earthq. Struct.*, **16**(6), 743-755. <https://doi.org/10.12989/eas.2019.16.6.743>.
- Warn, G.P., Whittaker, A.S. and Constantinou, M.C. (2007), "Vertical stiffness of elastomeric and lead-rubber seismic isolation bearings", *J. Struct. Eng.* **133**, 1227-1236. [http://dx.doi.org/10.1061/\(ASCE\)0733-9445\(2007\)133:9\(1227\)](http://dx.doi.org/10.1061/(ASCE)0733-9445(2007)133:9(1227)).
- Xiong, W., Zhang, S.J., Jiang, L.Z. and Li, Y.Z. (2017), "Introduction of the convex friction system (CFS) for seismic isolation", *Struct. Cont. Hlth. Monit.*, **24**(1), 1861. <https://doi.org/10.1002/stc.1861>.
- Xiong, W., Zhang, S.J., Jiang, L.Z. and Li, Y.Z. (2018), "The multangular-pyramid concave friction system (MPCFS) for seismic isolation: A preliminary numerical study", *Eng. Struct.*, **160**, 383-394. <https://doi.org/10.1016/j.engstruct.2017.12.045>.
- Yamamoto, S., Kikuchi, M., Ueda, M. and Aiken, I.D. (2009), "A mechanical model for elastomeric seismic isolation bearings including the influence of axial load", *Earthq. Eng., Struct. Dyn.*, **38**, 157-180. <https://doi.org/10.1002/eqe.847>.
- Zayas, V.A., Low, S.S. and Mahin, S.A. (1990), "A simple pendulum technique for achieving seismic isolation", *Earthq. Spectra*, **6**(2), 317-33. <https://doi.org/10.1193%2F1.1585573>.

CC